Copper(II) Benzoate Nitroxide Dimers and Chains: Structure and Magnetic Studies†

Rico E. Del Sesto, Atta M. Arif, and Joel S. Miller*

Department of Chemistry, 315 South 1400 East Room 2124, University of Utah, Salt Lake City, Utah 84112-0850

Received June 27, 2000

Copper(II) benzoate dimers and linear chains have been synthesized and exhibit very different magnetic behaviors. The benzoate dimers, **1a**, show typical dimeric singlet−triplet transitions and strong antiferromagnetic coupling ($J_{ST} = -206$ K (-143 cm^{-1}); $H = -2J_{ST}\mathbf{S}_a\cdot\mathbf{S}_b$). The bromobenzoate dimer can be converted into linear chains of hydrogen-bonded monomers, showing 1-D ferromagnetic coupling (**6a**, $\theta = +9$ K). Copper(II) sites can also be bridged by nitroxide-substituted benzoates, **1b** and **1c**, that is, 2-(4′-carboxyphenyl)-4,4,5,5-tetramethylimidazoline-3-oxide-1-oxyl (NNBA, **3a**), with $J_{ST} = -216$ K (-150 cm^{-1}), with comparable interactions between the nitroxide and triplet Cu(II) spins, $\theta_T = -157$ K. A 1-D chain similar to the bromobenzoate monomers can also be produced with NNBA, also exhibiting ferromagnetic coupling (**6b**, $\theta = +0.67$ K), albeit much weaker. Other nitroxides have been introduced into the Cu(II) dimer system by capping copper(II) acetate with the polydentate 2-(4′-pyridyl)-4,4,5,5-tetramethylimidazoline-3-oxide-1-oxyl (PYNN, **3b**), which exhibits almost no coupling to the copper centers when both ends of the dimer are capped (**1d**, $\theta = -5.8$ K). In contrast, strong coupling is observed when only one PYNN is used (**2**, $\theta = -300$ K), which is the result of direct coordination of the nitroxide to the copper centers, producing a chain of the dimer units.

Introduction

A wide variety of spin-bearing compounds have been studied enroute to the development of room-temperature molecule-based magnets.[1] From the discovery of the $[Fe(C_5Me_5)_2][TCNE]$[2] (TCNE = tetracyanoethylene) magnets[3] to the dithiadiazolyl radical-based weak ferromagnet,[4] the approach to understanding magnetism has covered organometallic and purely organic-based materials. Because of the embryonic nature of organic-based magnets, there is still much to learn about the fundamental spin-coupling behavior from the studies of all compounds, whether they exhibit ferro-, ferri-, or antiferromagnetic coupling or ordering.

One of the oldest magnetic systems studied is the carboxylate-bridged copper(II) dimers, $[Cu^{II}(O_2CR)_2]_2$ (**1**). The $S = {}^1/_2$ Cu^{II} atoms exhibit strong intradimer antiferromagnetic coupling due to superexchange via the carboxylate bridge,[5] producing a singlet ground state ($S_{tot} = 0$) and a thermally populated triplet ($S_{tot} = 1$) excited state, and the susceptibility, χ, can be modeled using the Bleaney−Bowers expression (eq 1) for $H = -2J_{ST}\mathbf{S}_a\cdot\mathbf{S}_b$:[6]

$$\chi_{BB} = \frac{2Ng^2\beta^2}{kT[3 + e^{-2J_{ST}/kT}]} \quad (1)$$

where N is Avogadro's number, g is the Lande g-value, β is the Bohr magneton, k is the Boltzmann constant, and J_{ST} is the

† Dedicated to the memory of Leigh C. Porter (October 29, 1955−May 13, 1999).

(1) (a) Ovcharenko, V. I.; Sagdeev, R. Z. *Russ. Chem. Rev.* **1999**, *68*, 345. (b) Kinoshita, M. *Philos. Trans. R. Soc. London, Ser. A* **1999**, *357*, 2855. (c) Miller, J. S.; Epstein, A. J. *Chem. Commun.* **1998**, 1319. (d) Plass, W. *Chem.-Ztg.* **1998**, *32*, 323. (e) Day, P. *J. Chem. Soc., Dalton Trans.* **1997**, 701. (f) Miller, J. S.; Epstein, A. J. *Chem. Eng. News* **1995**, *73*, No. 40, 30. (g) Miller, J. S.; Epstein, A. J. *Adv. Chem. Ser.* **1995**, *245*, 161. (h) Miller, J. S.; Epstein, A. J. *Angew. Chem., Int. Ed. Engl.* **1994**, *33*, 385. (i) Kahn, O. *Adv. Inorg. Chem*. **1995**, *43*, 179. (j) Kinoshita, M. *Jpn. J. Appl. Phys.* **1994**, *33*, 5718. (k) Gatteschi, D. *Adv. Mater.* (*Weinheim, Ger.*) **1994**, *6*, 635. (l) Kahn, O. *Molecular Magnetism*; VCH Publishers: New York, 1993. (m) Caneschi, A.; Gatteschi, D.; Rey, P. *Prog. Inorg. Chem.* **1991**, *39*, 331. (n) Buchachenko, A. L. *Russ. Chem. Rev.* **1990**, *59*, 307. (o) Caneschi, A.; Gatteschi, D.; Sessoli, R.; Rey, P. *Acc. Chem. Res.* **1989**, *22*, 392. (p) Miller, J. S.; Epstein, A. J. In *New Aspects of Organic Chemistry*; Yoshida, Z., Shiba, T., Oshiro, Y., Eds.; VCH Publishers: New York, 1989; p 237. (q) Miller, J. S.; Epstein, A. J.; Reiff, W. M. *Acc. Chem. Res.* **1988**, *21*, 114. (r) Miller, J. S.; Epstein, A. J.; Reiff, W. M. *Science* **1988**, *240*, 40. (s) Miller, J. S.; Epstein, A. J.; Reiff, W. M. *Chem. Rev.* **1988**, *88*, 201. (t) Kahn, O. *Struct. Bonding* **1987**, *68*, 89.

(2) (a) Miller, J. S.; Calabrese, J. C.; Epstein, A. J.; Bigelow, R. W.; Zhang, J. H.; Reiff, W. M. *J. Chem. Soc., Chem. Commun.* **1986**, 1026. (b) Miller, J. S.; Calabrese, J. C.; Rommelmann, H.; Chittipeddi, S. R.; Zhang, J. H.; Reiff, W. M.; Epstein, A. J. *J. Am. Chem. Soc.* **1987**, *109*, 769. Chittipeddi, S.; Cromack, K. R.; Miller, J. S.; Epstein, A. J. *Phys. Rev. Lett.* **1987**, *58*, 2695.

(3) (a) Manriquez, J. M.; Yee, G. T.; McLean, R. S.; Epstein, A. J.; Miller, J. S. *Science* **1991**, *252*, 1415. Miller, J. S.; Yee, G. T.; Manriquez, J. M.; Epstein, A. J. In *Conjugated Polymers and Related Materials*: *The Interconnection of Chemical and Electronic Structure*, Proceedings of Nobel Symposium No. NS-81; Oxford University Press: 1993; p 461. *Chim. Ind.* (*Milan*) **1992**, *74*, 845. Epstein, A. J.; Miller, J. S. In *Conjugated Polymers and Related Materials*: *The Interconnection of Chemical and Electronic Structure*, Proceedings of Nobel Symposium No. NS-81; Oxford University Press: 1993; p 475. *Chim. Ind.* (*Milan*)-**1993**, *75*, 185. (b) Zhang, J.; Zhou, P.; Brinckerhoff, W. B.; Epstein, A. J.; Vazquez, C.; McLean, R. S.; Miller, J. S. *ACS Symp. Ser*. **1996**, *644*, 311.

(4) (a) Banister, A. J.; Bricklebank, N.; Lavender, I.; Rawson, J. M.; Gregory, C. I.; Tanner, B. K.; Clegg, W.; Elsegood, M. R. J.; Palacio, F. *Angew. Chem., Int. Ed.* **1996**, *35*, 2533. (b) Banister, A. J.; Bricklebank, N.; Clegg, W.; Elsegood, M. R. J.; Gregory, C. I.; Lavender, I.; Rawson, J. M.; Tanner, B. K. *J. Chem. Soc., Chem. Commun.* **1995**, 679.

(5) Carlin, R. L. *Magnetochemistry*; Springer-Verlag: New York, 1986; p 82.

(6) Bleaney, B.; Bowers, K. D. *Proc. R. Soc. London, Ser. A* **1952**, *214*, 451.

10.1021/ic0007106 CCC: $19.00
Published on Web 09/28/2000

intradimer coupling (with $J_{ST} < 0$ indicating antiferromagnetic interactions, and therefore the triplet state is higher in energy than the singlet state). These properties are also observed for axially ligated $[Cu^{II}(O_2CR)_2]_2$ dimers, that is, $[Cu^{II}(O_2CR)_2]_2L_2$ (L = H_2O, pyridine, 2-picoline).[7] In contrast, isostructural $[M^{II}(O_2CR)_2]_2$ (M = Cr, Mo, Rh) dimers with their respective single and quadruple bonds exhibit strong antiferromagnetic coupling[8] and are diamagnetic at room temperature due to complete population of the $S = 0$ ground state, whereas $[Ru^{II}(O_2CR)_2]_2$ is $S = 1$ ($\sigma^2\pi^4\delta^2\pi^{*3}\delta^{*1}$)[9] and $[Ru^{II/III}(O_2CR)_2]_2^+$ has a $S = {}^3/_2$ ($\sigma^2\pi^4\delta^2\delta^{*2}\pi^{*1}$) ground state.[10]

Previous attempts to develop high-spin molecules via coupling to the thermally populated copper-dimer triplet with an $S = {}^1/_2$ nitroxide [e.g., TEMPO (2,2,5,5-tetramethylpiperidinyl-1-oxyl, **5**)[11]] were unsuccessful as strong antiferromagnetic interactions occur between the spins, leading to a net moment near zero.

Herein, we postulate that by (1) introducing the organic radicals into the equatorial position of a copper dimer as a substituent of the carboxylate bridge, that is, $[Cu^{II}(O_2CR)_2]_2L_2$ (R not L being spin bearing), or (2) weakening the strong Cu(II)−L (where L is spin bearing) antiferromagnetic coupling by increasing the distance of the spin-containing portion on L from the Cu(II), it may be possible that (a) isolated organic radicals as well as the singlet−triplet transition of the copper dimer are maintained and (b) these spins may ferromagnetically couple if the Cu(II) magnetic orbital ($d_{x^2-y^2}$) were orthogonal to those of R.[12] Furthermore, the extent of the perturbation of the superexchange mechanism through the carboxylate bridges may be studied if the organic spins are delocalized onto the carboxylate bridge.

To test these hypotheses, we targeted the preparation and study of $[Cu^{II}(\mathbf{3a})_2L]_2$ [**3a** = 2-(4′-carboxyphenyl)-4,4,5,5-tetramethylimidazoline-3-oxide-1-oxyl, NNBA] and $[Cu^{II}(O_2CMe)_2\mathbf{3b}]_2$ [**3b** = 2-(4′-pyridyl)-4,4,5,5-tetramethylimidazoline-3-oxide-1-oxyl, PYNN]. Because of the lack of direct coordination between the nitroxide spin center (i.e., O) and Cu(II), strong antiferromagnetic coupling between the nitroxide to the Cu(II) is prevented. Additionally, using only 1 equiv of **3b** should result in a linear chain linked by bridging **3b** as previously reported for $[Ru^{II/III}(O_2CCMe_3)_2]_2(L)$,[13a] [L = PYNN (**3b**) or 2-phenyl-,4,4,5,5-tetramethylimidazoline-4,5-dihydro-1*H*-imidazolyl-1-oxy, **4b**[13c]], and $[Rh^{II}(O_2CCF_3)_2]_2(L)$ (L = **4a** or 2,4,4,5,5-pentamethylimidazoline-4,5-dihydro-1*H*-imidazolyl-1-oxy 3-oxide, **4c**).[14a] In addition to these new compounds, chain compound **6** and the isolated monomer **7** were unexpectedly isolated and their characterization is reported.

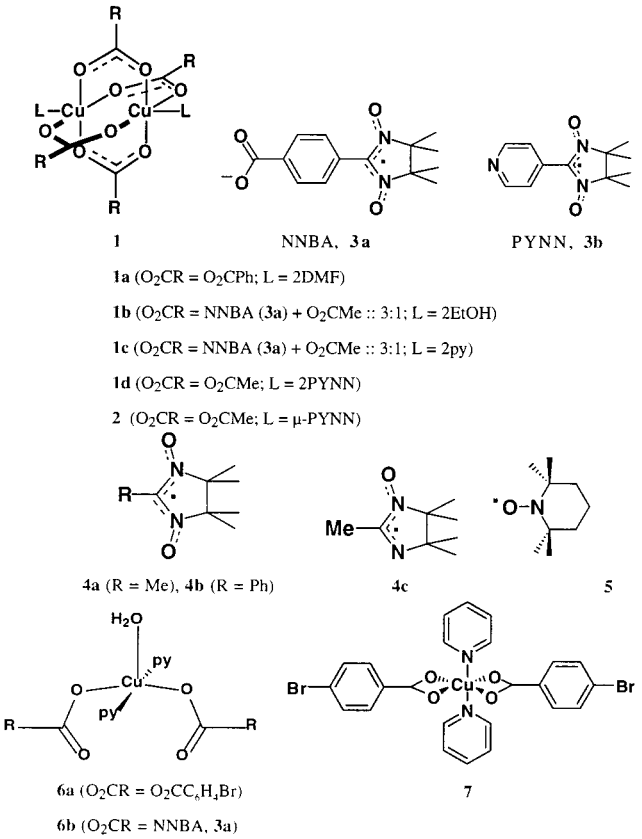

Experimental Section

Synthesis. All chemicals needed in the preparations of the studied samples were used as received. An infrared Bio-Rad FTS-40 FTIR spectrophotometer with ±1 cm^{-1} resolution was used. Samples were prepared either as Nujol mulls on NaCl plates or as KBr pressed pellets and were scanned in the wavenumber range of 400−4000 cm^{-1}.

Thermal properties and mass spectrometry were performed with a TA Instruments model 2050 thermal gravimetric analyzer (TGA), with the gas outlet connected to a TA Thermolab mass spectrometer, with ionization potential of 70 eV. Elemental analyses (C, H, and N) were carried out by Atlantic Microlabs (Norwalk, GA).

Magnetic susceptibility measurements were performed between 2 and 300 K at a field of 1000 Oe on a Quantum Design MPMS-5T SQUID magnetometer with a sensitivity of 10^{-8} emu as previously discussed.[15] Electron paramagnetic resonance (EPR) spectra were recorded using a Bruker EMX X-band spectrometer with 1,1-diphenyl-2-picrylhydrazyl (DPPH, Sigma) as an external standard ($g = 2.0037$). ^{1}H NMR measurements were performed on a Varian XL-300 with proton frequency at 300 MHz.

X-ray diffraction studies were made on a Nonius KappaCCD diffractometer equipped with Mo Kα (λ = 0.710 73 Å) radiation. Structures of **1a**, **6a**, and **7** (Table 1) were solved by direct methods using the program SIR-97 and were refined by the full-matrix least-squares method on F^2 with SHELXL 97.[16] Anisotropic thermal parameters were assigned to Cu, C, N, and O atoms, and hydrogen atoms and their positions were assigned using the Riding model. ORTEP

(7) (a) Harada, A.; Tsuchimoto, M.; Ohba, S.; Iwasawa, K.; Tokii, T. *Acta Crystallogr., Sect. B* **1997**, *53*, 654. (b) Mei, W.; Yu, X.; Na, Y.; Man, J. *Indian J. Chem.* **1997**, *36A*, 887. (c) Melník, M. *J. Inorg. Nucl. Chem.* **1979**, *41*, 779.
(8) Boudreaux, E. A.; Mulay, L. N. *Theory and Applications of Molecular Paramagnetism*; John Wiley and Sons: New York, 1976; p 406.
(9) (a) Lindsay, A. J.; Wilkinson, G.; Motevalli, M.; Hursthouse, M. B. *J. Chem. Soc., Dalton Trans.* **1985**, 2321. (b) Lindsay, A. J.; Wilkinson, G.; Motevalli, M.; Hursthouse, M. B. *J. Chem. Soc., Dalton Trans.* **1987**, 2723. (c) Cogne, A.; Belorizky, E.; Laugier, J.; Rey, P. *Inorg. Chem.* **1994**, *33*, 3364.
(10) Bino, A.; Cotton, F. A.; Felthouse, T. R. *Inorg. Chem.* **1979**, *18*, 2599.
(11) (a) Porter, L.; Dickman, M.; Doedens, R. *Inorg. Chem.* **1983**, *22*, 1962. (b) Porter, L.; Doedens, R. *Inorg. Chem.* **1985**, *24*, 1006. (c) Porter, L.; Dickman, M.; Doedens, R. *Inorg. Chem.* **1986**, *25*, 678. (d) Porter, L. Ph.D. Thesis, University of California, Irvine, CA, 1984.
(12) Luneau, D.; Rey, P.; Laugier, J.; Fries, P.; Caneschi, A.; Gatteschi, D.; Sessoli, R. *J. Am. Chem. Soc.* **1991**, *113*, 1245.
(13) (a) Sayama, Y.; Handa, M.; Mikuriya, M.; Hiromitsu, I.; Kasuga, K. *Chem. Lett.* **1998**, 777. (b) Sayama, Y.; Handa, M.; Mikuriya, M.; Hiromitsu, I.; Kasuga, K. *Chem. Lett.* **1999**, 453. (c) Handa, M.; Sayama, Y.; Mikuriya, M.; Hukada, R.; Hiromitsu, I.; Kasuga, K. *Bull. Chem. Soc. Jpn.* **1998**, *71*, 119.
(14) (a) Cogne, A.; Grand, A.; Rey, P.; Subra, R. *J. Am. Chem. Soc.* **1989**, *111*, 3230. (b) Cogne, A.; Grand, A.; Rey, P.; Subra, R. *J. Am. Chem. Soc.* **1987**, *109*, 7927.
(15) Brandon, E. J.; Rittenberg, D. K.; Arif, A. M.; Miller, J. S. *Inorg. Chem.* **1998**, *37*, 3376.
(16) (a) Sheldrick, G. M. *SHELX97-2 Programs for Crystal Structure Analysis*, (release 97-2); Institüt für Anorganische Chemie der Universität, Göttingen, Germany, 1998. (b) Farrugia, L. J. *J. Appl. Crystallogr.* **1997**, *30*, 565.

Table 1. Crystallographic Data Collection and Structure Refinement Parameters for $[Cu(O_2CPh)_2(DMF)]_2$ (**1a**), $[Cu(O_2CC_6H_4Br)_2Py_2]\cdot H_2O$ (**6a**), and $[Cu(O_2CPh)_2Py_2]$ (**7**)

	1a	**6a**	**7**
chemical formula	$C_{34}H_{34}N_2O_{10}Cu_2$	$C_{24}H_{20}N_2O_5Br_2Cu$	$C_{24}H_{18}N_2O_5Br_2Cu$
formula mass, Da	757.71	639.78	621.76
space group	$P2_1/n$	$C2$	$P\bar{1}$
a, Å	10.5055(2)	15.8610(9)	5.9662(2)
b, Å	10.0650(4)	5.8690(a)	8.1860(3)
c, Å	16.2460(5)	14.9720(8)	12.8681(5)
α, deg	90	90	94.1200(19)
β, deg	93.764(2)	121.3811(15)	99.512(2)
γ, deg	90	90	993.944(2)
V, Å^3	1714.11(9)	1189.85(10)	607.25(4)
ρ_{calcd}, mg/m^3	1.468	1.786	1.700
T, K	200(0.1)	200(0.1)	200(0.1)
λ, Å	0.71073	0.71073	0.71073
R1(F_o^2)^a =	0.0258	0.0221	0.0770
wR2(F_o^2)^b =	0.0720	0.0582	0.2413
Z	2	2	1
μ, mm^{-1}	1.299	4.315	4.222

^{a} $R1 = \sum(||F_o| - |F_c||)/\sum|F_o|$. ^{b} $wR2 = [\sum(w(F_o^2 - F_c^2)^2)/\sum(F_o^2)^2]^{1/2}$.

diagrams were generated using ORTEP 3.[16] Disorder was not observed in any of the structures.

2-(4′-Carboxyphenyl)-4,4,5,5-tetramethyl-1,3-dihydroxyimidazoline (NNBAH).[17] To a solution of 2,3-bis(hydroxyamine)-2,3-dimethylbutane (ACROS) (2.42 g, 0.010 mol) and sodium bicarbonate (0.020 mol) in water (30 mL) was added 4-carboxybenzaldehyde (Aldrich) (1.48 g, 0.010 mol) in small portions at 0 °C. The solution was allowed to stir for 48 h at room temperature. The resulting white precipitate was filtered, washed with cold water, and then dried in vacuo over P_2O_5 (yield: 2.04 g, 68%). IR, ν (Nujol): 3402m, 3181m, 1623m, 1592m, 1439s, 1260s, 1173s cm^{-1}. ^{1}H NMR (300 MHz, DMSO): 7.81 (s, 3H), 7.55−7.98 (dd, 4H), 4.60 (s, 1H), 1.09 (2s, 12H).

2-(4′-Carboxyphenyl)-4,4,5,5-tetramethylimidazoline-3-oxide-1-oxyl (NNBA), 3a.[17] To a suspension of NNBAH (510 mg, 1.68 mmol) in water (35 mL), a solution of sodium periodate (Aldrich) (600 mg, 2.80 mmol) in water (10 mL) was added, and the reaction mixture was allowed to stir at room temperature for 4 h. The deep blue precipitate was filtered out, resuspended in water, and extracted with ethyl acetate (4 × 75 mL). The ethyl acetate solution was then washed with water (4 × 50 mL), dried with magnesium sulfate, and then removed under reduced pressure. The resulting purple powder was then dried in vacuo over P_2O_5 (yield: 225 mg, 49%). IR ν (Nujol): 2928m, 1702w, 1355s (NO), 1313m, 1260m, 1171m, 1018w cm^{-1}. EPR (ethyl acetate, DPPH ref): $g_{(NO)} = 2.0013$, $A(^{14}N) = 0.79$ mT.

2-(4′-Pyridyl)-4,4,5,5-tetramethyl-1,3-dihydoxyimidazoline.[17] To a solution of 2,3-bis(hydroxyamine)-2,3-dimethylbutane (2.49 g, 11 mmol) and sodium bicarbonate (1.80 g, 22 mmol) in water (30 mL) was added 4-pyridinecarboxaldehyde (Aldrich) (1.1 mL, 1.122 g/mL, 0.012 mol) in small portions at 0 °C. The solution was allowed to stir for 40 h at room temperature. The resulting white precipitate was filtered, washed with cold water, and then dried in vacuo over P_2O_5 (yield: 1.05 g, 42%). ^{1}H NMR (300 MHz, DMSO): 7.95 (s, 2H), 7.45−8.52 (dd, 4H), 4.50 (s, 1H), 1.05 (2s, 12H).

2-(4′-Pyridyl)-4,4,5,5-tetramethylimidazoline-3-oxide-1-oxyl (PYNN), 3b.[17] The oxidation of the pyridine analogue was carried out in the exact same manner as for NNBAH (yield: 242 mg, 54%). IR ν (Nujol): 2946m, 1625s, 1427m, 1361s, 1290m, 1010m cm^{-1}. EPR (ethyl acetate, DPPH ref): $g_{(NO)} = 2.0014$.

$[Cu(O_2CPh)_2(DMF)]_2$, 1a. To a solution of $[Cu(O_2CMe)_2]_2\cdot 2H_2O$ (Aldrich) (4.0 g, 20 mmol) in warm mixed xylenes (100 mL, 45 °C) was added benzoic acid (6.1 g, 50 mmol). The solution was allowed to reflux (118 °C, bp for acetic acid) for 30 min, followed by heating at 130 °C for 4 h. After this time, the solution was allowed to cool to room temperature, and the resulting light blue precipitate was filtered and dried in vacuo. The product was dissolved in warm dimethylformamide (DMF) and allowed to cool slowly to 0 °C, upon which time green-blue crystals formed. IR ν (Nujol): 1757m, 1719s, 1617m, 1590m, 1252m, 1112w cm^{-1}.

$[Cu_2(NNBA)_3(O_2CMe)(EtOH)_2]$, 1b. $[Cu(O_2CMe)_2]_2\cdot 2H_2O$ (183 mg, 0.92 mmol) was dissolved in 100% ethanol (40 mL). A solution of *p*-NNBAH (550 mg, 1.98 mmol) in ethanol (75 mL) was added to the copper solution, and the mixture was stirred at room temperature for 20 h. The resulting deep blue precipitate was filtered out and dried in vacuo (yield: 530 mg, 89%). IR ν (Nujol): 3434w, 1676m, 1618s, 1560m, 1360s, 1308m, 1229m, 1171s cm^{-1}. Anal. Calcd for $C_{48}H_{64}N_6O_{16}Cu_2$: C, 52.03; H, 5.71; N, 7.58%. Found: C, 51.74; H, 5.78; N, 7.81%.

$[Cu_2(NNBA)_3(O_2CMe)py_2]$, 1c. To the ethanol-capped dimer, **1b**, suspended in methanol was added exactly 2 equiv of pyridine, and the mixture was allowed to stir for 10 min. The solvent was removed under reduced pressure until a precipitate appeared, resulting in deep blue powder. IR ν (Nujol): 1681w, 1623m, 1560m, 1366s, 1302w, 1224m, 1171m cm^{-1}. Anal. Calcd for $C_{54}H_{64}N_8O_{14}Cu_2$: C, 55.10; H, 5.44; N, 9.55%. Found: C, 54.71; H, 5.78; N, 9.91%.

$[Cu(O_2CMe)_2(PYNN)]_2$, 1d. To $[Cu(O_2CMe)_2]_2\cdot 2H_2O$ (85 mg, 0.22 mmol) in ethanol (10 mL) was added 2 equiv of *p*-PYNN (100 mg, 0.44 mmol) per dimer, and the mixture was stirred for 1 h at room temperature. The resulting deep blue powder was filtered and dried in vacuo (yield: 75 mg, 59%). IR ν (Nujol): 1623s, 1600s, 1550m, 1345s, 1306m, 1213m, 1166m cm^{-1}. Anal. Calcd for $C_{32}H_{44}N_6O_{12}Cu_2$: C, 46.21; H, 5.37; N, 10.10%. Found: C, 46.17; H, 5.51; N, 9.89%.

$[Cu(O_2CMe)_2(PYNN)]_2$, 2.[13] To $[Cu(O_2CMe)_2]_2\cdot 2H_2O$ (85 mg, 0.22 mmol) dissolved in ethanol (10 mL) was added 1 equiv of *p*-PYNN (50 mg, 0.22 mmol) per dimer, and the mixture was stirred for 1 h at room temperature. The resulting deep blue powder was filtered and dried in vacuo. IR ν (Nujol): 1631s, 1592m, 1535m, 1325m, 1201w, 1166w cm^{-1}.

$[Cu(O_2CC_6H_4Br)_2py_2]\cdot H_2O$, 6a, and $[Cu(O_2CC_6H_4Br)_2py_2]$, 7. These compounds were made according to the same procedure for the copper benzoate, using 4-bromobenzoic acid (Aldrich) instead of benzoic acid. Also, the products were crystallized from a mixture of DMF/pyridine (5:1), because the initial crude product would not dissolve in DMF alone. Both compounds cocrystallize from this solvent. IR ν (Nujol) **6a**: 3076s, 3018m, 1676m, 1602s, 1492s, 1118m, 1050s, 1024m cm^{-1}. The limited amount of **7** crystallized from solution was insufficient to carry out any characterization other than X-ray crystal structure. The crystals were separated by hand under a microscope in order to determine its structure.

$[Cu(NNBA)_2py_2]\cdot H_2O$, 6b. To the ethanol-capped dimer, **1b**, suspended in methanol was added exactly 2 equiv of pyridine, and the

(17) Ullman, E.; Osiecki, J.; Boocock, D.; Darcy, R. *J. Am. Chem. Soc.* **1972**, *94*, 7049.

mixture was allowed to stir for 12 h. The solvent was removed under reduced pressure until a precipitate appeared, resulting in deep blue powder. IR ν (Nujol): 3355w, 1602m, 1355s, 1302m, 1218w, 1172m cm^{-1}. Anal. Calcd for $C_{38}H_{46}N_6O_9Cu$: C, 57.46; H, 5.84; N, 10.58%. Found: C, 56.52; H, 5.58; N, 10.41%.

X-ray Crystal Structure Analysis. Crystallographic data (excluding structure factors) for the structure reported herein have been deposited with the Cambridge Crystallographic Data Centre as supplementary publication no. CCDC-143665 (**1a**), CCDC-143666 (**6a**), and CCDC-143667 (**7**). Copies of the data can be obtained free of charge on application to The Director, CCDC, 12 Union Road, Cambridge CB2 1EZ, U.K. (fax: int code + (1223) 336 033; e-mail: deposit@ccdc.cam.ac.uk).

Results and Discussion

Synthesis. (a) $[Cu(O_2CC_6H_4X)_2L]_2$. The model compound $[Cu(O_2CPh)_2]_2$ was synthesized by refluxing $[Cu(O_2CMe)_2(OH_2)]_2$ with benzoic acid at 118 °C in xylenes, boiling off acetic acid as the reaction progressed. This synthesis was developed in order to drive the reaction in favor of the products, as material of reasonable purity in practical yields could not be obtained using known syntheses.[18] Typical syntheses of the dimers involve the reaction of Cu(II) salts with the corresponding carboxylic acid and a coordinating ligand (e.g., py); however, high-purity materials were difficult to obtain from these reactions.

The reaction in refluxing xylenes forms the linear chain of copper monomers similar to those previously reported,[19] which upon dissolution in DMF forms the DMF-capped dimers, **1a**. In contrast, using 4-bromobenzoic acid the initial linear chain product did not redissolve in DMF but did dissolve in 5:1 DMF/pyridine solution. Upon standing at room temperature, two different products cocrystallized: (1) deep-blue crystals, **6a**, of composition $[Cu(O_2CC_6H_4Br)_2py_2(OH_2)]$ and (2) a purple crystalline coproduct, **7**, of composition $[Cu(O_2CC_6H_4Br)_2py_2]$, both of which were structurally determined.

(b) $[Cu_2(O_2CMe)(NNBA)_3(EtOH)_2]$. To prevent decomposition of the radical-based ligands at elevated temperatures, $[Cu(O_2CMe)_2(OH_2)]_2$ was stirred with the NNBAH in absolute ethanol for 1 day at room temperature. The deep blue color of the precipitate was consistent with a dimeric structure that was confirmed from its magnetic behavior (vide infra). On the basis of infrared spectra, the nitroxide was still present, as evidenced by the 1360 cm^{-1} peak assigned to the ν_{NO}.[17] The expected percent composition predicted for the anticipated $[Cu(NNBA)_2(EtOH)]_2$ (C, 54.41; H, 5.29; N, 8.46%) was at variance with the observed values (C, 51.73; H, 5.82; N, 7.81%), and quantitative agreement of the magnetic data could not be obtained. Hence, this expected composition was deemed incorrect, and using a computer analysis[20] the composition was determined to be $[Cu_2(O_2CMe)(NNBA)_3(EtOH)_2]$ (**1b**) (C, 52.07; H, 5.69; N, 7.59%). This unexpected composition also enabled the quantitative fitting of the magnetic data (vide infra). TGA-MS also supports the presence of both acetate and NNBA ligands in **1b**. In the thermal analysis of **1b**, decomposition is seen at ~200 °C, with loss of both ethanol (46 amu) and acetate (60 amu). A second decomposition at 290 °C, when the NNBA ligand began to decompose, was also observed (Table 2). For comparison, $[Cu(O_2CMe)_2(OH_2)]_2$ begins to decompose at ~300 °C, with the fragments lost containing mass values of 44 (carbon dioxide) and 60 amu (acetic acid). NNBAH shows decomposition at ~215 °C, with formation of fragments with mass values of 44 (CO_2) and 60 amu (HOAc), and a second loss of mass at 300 °C with mass values of 44, 76, 103, and 104 amu. These peaks correspond to loss of carbon dioxide, C_6H_4, $C_6H_4C{=}NH$, and $C_6H_4C{=}NH_2$. The reaction of **1b** in methanol with exactly 2 equiv of pyridine resulted in the pyridine-capped dimer **1c**. The TGA-MS, showing peaks for pyridine, acetate, and NNBA fragments, and the magnetic properties (vide infra) support this structure. However, if the solution is allowed to stir for 12 h, a product similar to that of the linear chain of the bromobenzoate monomers is believed to result, in which two NNBA ligands, two pyridines, and one water molecule create the square-pyramidal environment around the copper center, **6b**. Elemental analysis agrees with this monomeric form, and IR shows that the nitroxide is still present with the ν_{NO} stretch at 1355 cm^{-1}. The magnetic data also show ferromagnetic coupling similar to that of **6a** (vide infra).

Table 2. Summary of TGA-MS Fragment Loss

compound	decomposition T (°C)	fragments lost, mass (amu)
$Cu_2(O_2CMe)_4(H_2O)_2$	300	44, 60
1a	295	44, 58, 76
1b	200	46, 60
	290	44, 76, 103, 104
1c	270	44, 60, 76, 79, 103, 104
3a	215	44, 58, 60
	300	60, 76, 103, 104

(c) $[Cu(O_2CMe)_2]_2(PYNN)_x$. In the attempts to place the nitroxide radical distant from the Cu(II) centers in the apical position, $[Cu(O_2CMe)_2]_2{\cdot}2H_2O$ was dissolved in ethanol and 2 equiv of PYNN per copper dimer was added, expecting the pyridyl N of the PYNN to be the strongest donor atom and thus to displace ethanol and water. This resulted in discrete bis-PYNN-capped copper acetate dimers **1d**, as suggested by elemental analysis, the presence of the nitroxide stretch in the IR, and magnetic properties. In contrast, reaction of only 1 equiv of PYNN with the $[Cu(O_2CMe)_2]_2$ results in the formation of $[Cu(O_2CMe)_2]_2$ (PYNN), which is assigned to be a chain of copper dimers linked by the bridging PYNN ligands, as evidenced by the shift of the ν_{NO} bands from 1345 to 1325 cm^{-1}. Hence, the copper dimers could be bridged by a PYNN with a pyridyl N and nitroxide O bound to each dimer forming a uniform chain, **2a**. This motif has been reported for $[Ru^{II/III}(O_2CCMe_3)_2]_2(PYNN)$[13] and $[Rh^{II}(O_2CMe_3)_2]_2(L)$ (L = **4c**).[14] Alternatively, a chain can form with one copper dimeric unit axially coordinated to two pyridyl moieties while the adjacent dimeric unit is axially coordinated by two nitroxide groups, producing a nonuniform chain of dimers, **2b**.[21] This motif has been very recently reported for $[Cu^{II}(O_2CCMe_3)_2]_2(m\text{-PYNN})$[21a] as well as $[Ru^{II/III}(O_2CCMe_3)_2]_2(L)$ (L = **4a**,[13b] **5**[22]). Either **2a**

(18) (a) Bateman, W.; Conrad, D. *J. Am. Chem. Soc.* **1915**, *37*, 2553. (b) Lewis, J.; Lin, Y.; Royston, L.; Thompson, R. *J. Chem. Soc.* **1965**, 6464. (c) van Niekerk, J.; Schoening, F. *Acta Crystallogr.* **1953**, *6*, 227.

(19) (a) Deakin, L.; Arif, A. M.; Miller, J. S. *Inorg. Chem.* **1998**, *38*, 5072. (b) Bakalbassis, E.; Bergerat, P.; Kahn, O.; Jeannin, S.; Jeannin, Y.; Dromzee, Y.; Guillot, M. *Inorg. Chem.* **1992**, *31*, 625.

(20) Miller, J. S.; Goedde, A. O. *J. Chem. Educ.* **1975**, *50*, 43; *Quant. Chem. Prog. Exch.* **1976**, *10*, 299.

(21) (a) Chung, Y.-H.; Wei, H.-H. *Inorg. Chem. Commun.* **1999**, *2*, 269. (b) The authors report attempting to fit their susceptibility data using a nonuniform chain, resulting in a poor fit. However, we believe that this model would be inappropriate for our compound **2** as the nonuniform chain model is for interacting ($S = 1/2$)−($S = 1/2$) systems, which is not consistent with the ($S = 1/2$ (nitroxide))−($S = 1$) copper dimer systems we are studying.

(22) Handa, M.; Sayama, Y.; Mikuriya, M.; Hiromitsu, I.; Kasuga, K. *Bull. Chem. Soc. Jpn.* **1995**, *68*, 1647.

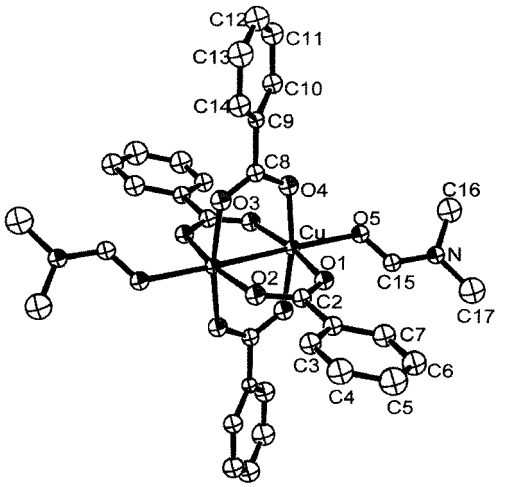

Figure 1. ORTEP (50% electron density) and atom labeling diagram for $[Cu(O_2CPh)_2(DMF)]_2$, **1a**, with a Cu···Cu distance of 2.63 Å.

or **2b** results in direct Cu(II)−nitroxide interactions and thus a large antiferromagnetic coupling (vide infra).

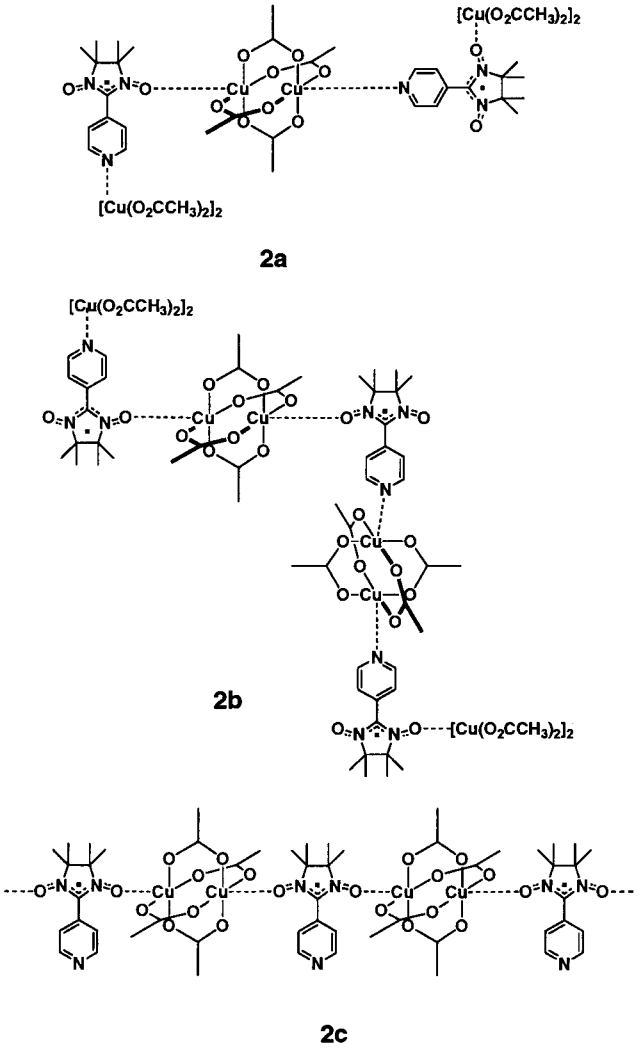

Structures. $[Cu(O_2CC_6H_4X)_2L]_2$. The structure of the $[Cu(O_2CPh)_2(DMF)]_2$ (**1a**) model compound was determined. The intradimer Cu(II)···Cu(II) distance is 2.63 Å, which is very similar to 2.64 Å in copper(II) acetate.[18] The angle of the plane of the benzene ring to that of the copper−carboxylate plane is twisted by 35° (Figure 1). In the attempt to produce the

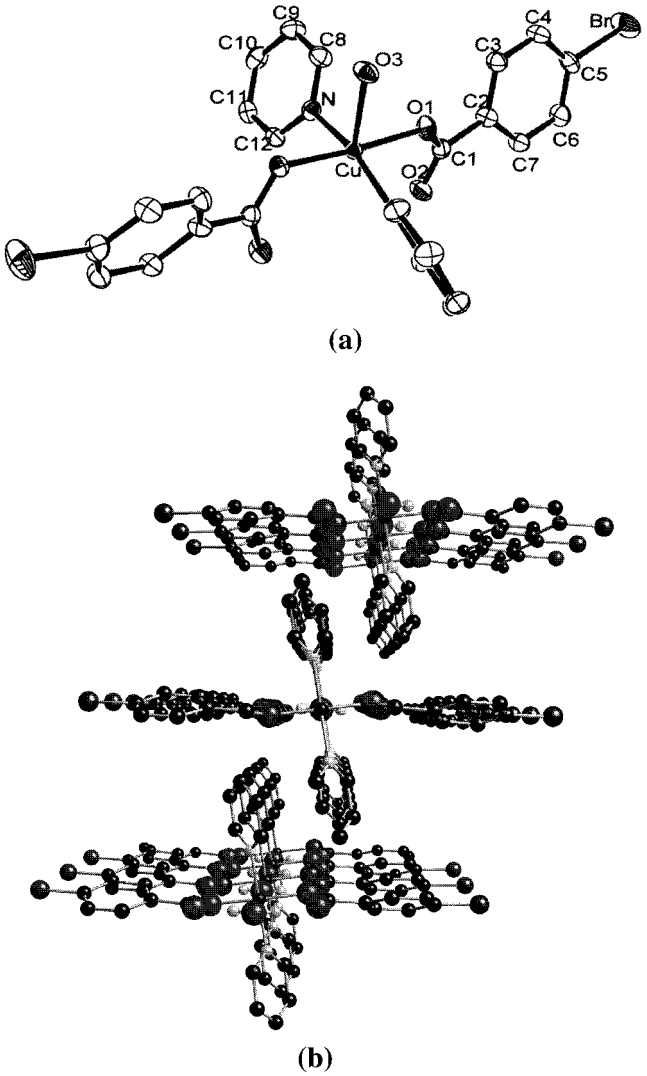

Figure 2. (a) ORTEP (50% electron density) and atom labeling diagram for $[Cu(O_2CPh)_2py_2]\cdot H_2O$, **6a**; (b) looking approximately down the *b* axis of **6a**.

bromobenzoate analogue of **1a**, two other products cocrystallized from the solution. The first was determined to be a linear chain of psuedo-square-pyramidal copper centers, with *trans*-benzoate and *trans*-pyridine ligands and one water molecule, **6a** (Figures 2and 3). The CuO, $CuO3_{H_2O}$, and CuN distances are 1.94, 2.20, and 1.98 Å, respectively, and the O3−Cu−N and O3−Cu−O1 angles are 98.9 and 87.5°, respectively. The water hydrogen bonds (1.98 Å) between the water of one monomer and the carboxylate of the adjacent monomer form linear chains (Figure 3). The second bromobenzoate product was an anhydrous pseudo-octahedral $[Cu^{II}(O_2CC_6H_4Br)_2py_2]$ complex (**7**). There is a center of inversion about the Cu(II) (Figure 4), with two bromobenzoate ligands creating a plane about the copper center. The oxygens of the carboxylates are asymmetrically coordinated to the copper center, with distances from the copper of 1.97 (Cu−O1) and 2.55 Å (Cu−O2). Pyridine occupies both apical positions, with the Cu−N distance of 2.01 Å.

Magnetic Properties. (a) $[Cu(O_2CC_6H_4Br)_2py_2]\cdot H_2O$. The susceptibility, χ, of the ligands **3a** and **3b** as well as those of the monomeric copper(II) complexes can be modeled by the Curie−Weiss expression, eq 2. The $S = {}^1/_2$ nitroxide ligands are magnetically well behaved with Weiss constants, θ, of −3.5

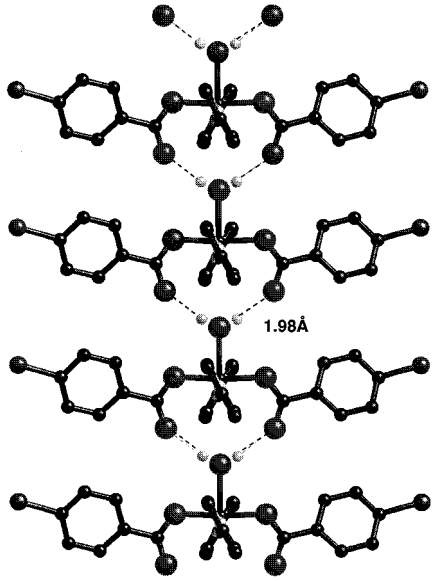

Figure 3. Hydrogen bonding structure of $[Cu(O_2CPh)_2py_2]\cdot H_2O$, **6a**.

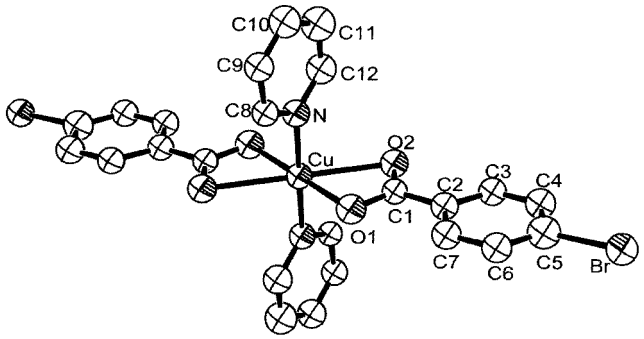

Figure 4. ORTEP (50% electron density) and atom labeling diagram for $[Cu(O_2CPh)_2py_2]$ (**7**).

$\pm$ 0.3 K and $g_{org} = 2.00$, characteristic of weak antiferromagnetic coupling between radicals in the solid state.

$$\chi_{CW} = \frac{Ng^2\beta^2 S(S+1)}{3k(T-\theta)} \qquad (2)$$

$[Cu(O_2CC_6H_4Br)_2py_2]\cdot H_2O$. The Cu(II) complexes, **6a** and **6b**, obey the Curie−Weiss expression above 30 K with $g_{Cu} = 2.16$ and $\theta = +9$ and 0.7 K, respectively (Figure 5). The relatively high θ value for **6a** suggests significant ferromagnetic coupling arising from the 1-D chains, and this is the subject of further study.

$[Cu(O_2CC_6H_4X)_2L]_2$, 1a. The magnetic susceptibility typical for copper dimers is exhibited by **1a**, where the triplet state is increasingly thermally populated with increasing temperature with $\chi(T)$ reaching a maximum around 230 K (Figure 6). The large increase in χ at very low temperatures is attributed to a small fraction (ρ) of the monomeric $S = {}^1/_2$ Cu(II) spin impurity being present,[23] and the total χ can be modeled by adding in a Curie component (eq 2) for that fraction of the impurity to eq 1, resulting in eq 3. Using $H = -2J_{ST}\mathbf{S}_a\cdot\mathbf{S}_b$, a fit to the observed data for **1a** has $J_{ST} = -206$ K (-143 cm^{-1}),[24] $g_{Cu} = 2.16$, and $\rho = 0.05$, which is comparable to $[Cu(OAc)_2]_2$ [$J_{ST} = -213$ K

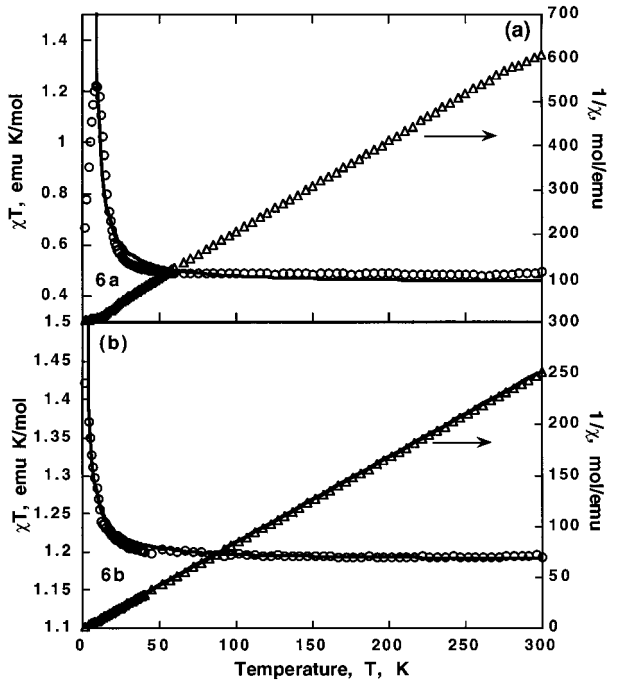

Figure 5. χT(T) and $1/\chi$(T) for (a) $[Cu(O_2CPh)_2py_2]\cdot H_2O$, **6a**, with $g_{Cu} = 2.16$ and $\theta = +9$ K and (b) $[Cu(NNBA)_2py_2]\cdot H_2O$, **6b**, with $g_{Cu} = 2.16$, $g_{org} = 2.001$, and $\theta = +0.7$ K.

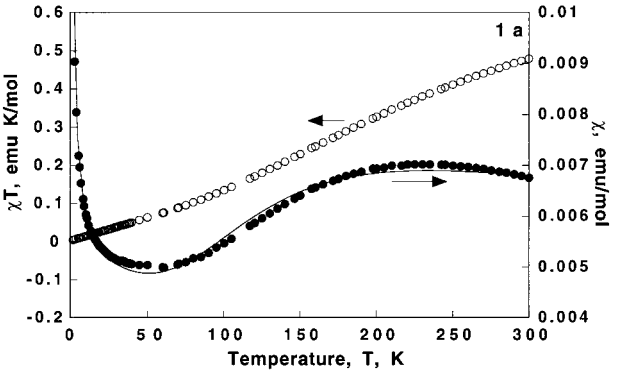

Figure 6. χT(T) (○) and χ(T) (●) for $[Cu(O_2CPh)_2(DMF)]_2$, **1a**. Fit to eq 3 with $J_{ST} = -206$ K (-143 cm^{-1}), $g_{Cu} = 2.16$, and $\rho = 0.05$.

(-148 cm^{-1}), $g_{Cu} = 2.09$, and $\rho = 0.0085$)].[23,25]

$$\chi = \frac{2Ng^2\beta^2}{kT[3 + e^{-2J_{ST}/kT}]}(1-\rho) + \frac{Ng^2\beta^2}{2kT}\rho \qquad (3)$$

$[Cu_2(O_2CMe)(NNBA)_3L_2]$, 1b, 1c. By modification of the substituents of the copper benzoate dimers with organic radicals, for example, NNBA (**3a**), the Bleaney−Bowers equation, eq 1, is not sufficient to account for the introduction of the organic radicals onto the dimer. The data can be fit to a summation of Curie−Weiss equation (2) for each quantum spin (due to the organic radicals, eq 2), and the Bleaney−Bowers equation (1) for the copper singlet−triplet dimer, resulting in eq 4, where n is the number of organic radicals per dimer and J_{ST} is the intradimer spin coupling between the singlet−triplet states of the copper dimer. The $e^{-2J/kT}$ term accounts for the population of the triplet state. The middle term of eq 4 reflects the intermolecular coupling, θ_S, between the $S = {}^1/_2$ organic radicals via either the singlet state of the copper dimer, which is

(23) Kahn, O. *Molecular Magnetism*; VCH Publishers: New York, 1993; p 107.
(24) J values are reported in cm^{-1} or as J/k in units of K.
(25) Felthouse, T. R.; Dong, T.-Y.; Hendrickson, D. N.; Shieh, H.-S.; Thompson, M. R. *J. Am. Chem. Soc.* **1986**, *108*, 8201.

Table 3. Summary of Magnetic Data

complex	g_{Cu}	g_{org}	J_{ST}, K (cm^{-1})	θ_S, K (cm^{-1})	θ_T, K (cm^{-1})	eq
$[Cu^{II}(O_2CMe)_2]_2 \cdot 2H_2O$ **23**·**25**	2.16		−213 (−148)			3
1a	2.16		−206 (−143)			3
1b	2.18	2.001	−216 (−150)	−1.5 (−1.0)	−157 (−109)	4
1c	2.18	2.001	−216 (−150)	−1.8 (−1.3)	−169 (−117)	4
1d	2.18	2.001	−223 (−155)	−5.8 (−4.0)	−5.8 (−4.0)	4
2	2.18	2.001	−238 (−165)	−5.9 (−4.1)	−300 (−205)	4
3a		2.0013		−3.8 (−2.7)		2
3b		2.0014		−3.2 (−2.2)		2
6a	2.16			+9 (+6.4)		2
6b	2.16	2.001		+0.7 (+0.5)		2
$[Cu^{II}(O_2CCCl_3)_2]_2$(**5**)[11b] [c]					very large[a]	
$[Cu^{II}(O_2CCCl_3)_2]_2$(*m*-**3b**)[11b] [c]	2.00	2.00	−253 (−176)	−2.0 (−1.4)		3
$[Ru^{II}(O_2CCF_3)_2$(**5**)$]_2$[9c]	2.00	2.00			−379 (−263)	ref 9c
$[Ru^{II}(O_2CC_6F_5)_2$(**5**)$]_2$[9c]	2.00	2.00			−337 (−234)	ref 9c
$[Ru^{II/III}(O_2CCMe_3)_2]_2$(**3b**)[13a]	2.23	2.00		−0.3 (0.45)	14 (20)	*b*
$[Ru^{II/III}(O_2CCMe_3)_2$(**5**)$]$[21]	2.117				−187 (−130)	ref 26
$[Ru^{II/III}(O_2CCMe_3)_2]_2$(**4b**)[13c] [c]	2.00	2.00			−144 (−100)	ref 13c
$[Ru^{II/III}(O_2CCMe_3)_2$(**4a**)$]$[13b]	2.20	2.00		−35 (−50)	14 (20)	*b*
$[Mo^{II}(O_2CCF_3)_2$(**5**)$]_2$[25]		2.00		−0.2 (−0.14)	very large[a]	2
$[Rh^{II}(O_2CCF_3)_2$(**5**)$]_2$[25]		2.00		−344 (−239)		1
$[Rh^{I}I(O_2CC_3F_7)_2$(**5**)$]_2$[25]		2.00		−387 (−269)		1
$[Rh^{II}(O_2CC_6F_5)_2$(**5**)$]_2$[25]		2.00		−265 (−184)		1
$[Rh^{II}(O_2CCF_3)_2$(**4b**)$]_2$[14a]		1.998		−120 (−83.6)		1
$[Rh^{II}(O_2CCF_3)_2]_2$(**4a**)[14a] [c]		2.114		−142 (−98.8)		
$[Rh^{II}(O_2CCF_3)_2$(**4c**)$]_2$[14a]		1.976		−11.8 (−5.2)		1
$[Rh^{II}(O_2CCF_3)_2]_2$(**4c**)[14a] [c]		2.122		3.3 (2.3)		ref 14a

[a] Diamagnetic. [b] Unknown. [c] Extended structure similar to that of **2**.

essentially completely populated at low temperature, or through-space either inter- or intramolecularly. The right-hand term of eq 4 reflects the intramolecular coupling, θ_T, between the organic radicals and the triplet state of the copper dimer, which is appreciably populated at higher temperatures (e.g., ∼20% at room temperature). Both θ_T and θ_S along with J_{ST} are determined from a fit of the data to eq 4.

$$\chi = \frac{2Ng_{Cu}{}^2\beta^2}{kT[3 + e^{(-2J_{ST}/kT)}]} + n\left[1 - e^{(-2J/kT)}\frac{Ng_{org}{}^2\beta^2S(S+1)}{3kT(T-\theta_S)} + e^{(-2J/kT)}\frac{Ng_{org}{}^2\beta^2S(S+1)}{3kT(T-\theta_T)}\right] \quad (4)$$

When three NNBA radicals are positioned equatorially around the copper dimer in **1b**, the susceptibility can be fit between 2 and 300 K with eq 4 with $n = 3$, $g_{Cu} = 2.18$, $g_{org} = 2.001$, $J_{ST} = -216$ K (−150 cm^{-1}), $\theta_S = -1.5$ K, and $\theta_T = -157$ K (Table 3, Figure 7a). Only unacceptably poor fits are obtained for $n = 2$ or 4, consistent with the formulation of the composition of **1b** as $[Cu_2(O_2CMe)(NNBA)_3(EtOH)_2]$ (vide supra). The intradimer Cu−Cu coupling (J_{ST}) of −150 cm^{-1} shows little perturbation from the presence of the nitroxide, as J_{ST} is essentially the same as that of **1a** (−143 cm^{-1}). The small value of the nitroxide−nitroxide spin coupling ($\theta_S \approx -1.5$ K) is attributed to either weak intermolecular nitroxide−nitroxide interactions or weak intramolecular nitroxide−nitroxide coupling via the singlet state of the copper dimer and is typical of nitroxides, for example, **3a** and **3b**. However, poor intradimer nitroxide coupling is expected because the pathway necessary for interaction would be through the copper dimer in the singlet state. Also, similar values (ca. −5 K) have been reported for nitroxide−nitroxide intermolecular interactions in other metal−nitroxide compounds, suggesting further that the low-temperature interactions are solely intermolecular.[14] In contrast, the large negative θ_T value of −157 K reflects strong antiferromagnetic coupling between the $S = 1/2$ nitroxide ligand and the triplet state of the copper dimer. When the ethanol capping ligands of **1b** are replaced by pyridine ligands, again two products result depending on the reaction time. The pyridine-capped dimer structure, **1c**, shows similar magnetic behavior to that of **1b** (Figure 7b), with the same coupling between the copper centers ($J_{ST} = -150$ cm^{-1}) and small changes in the

(26) A separate model which the authors unsuccessfully attempted to fit the data was for an ($S = 1/2$)−($S = 1$)−($S = 1/2$) trimer, where the $S = 1$ is the copper dimer at room temperature and the two $S = 1/2$ spins are for the axially bound nitroxides. For the $[Cu_2(O_2CMe)_4(PYNN)]_2$ system, **1d**, the following model was attempted:

$$\chi_{total} = \chi_{BB} + [(1 - e^{-2(J_{ST}/kT)})\chi_{j_1}] + [(e^{-2(J_{ST}/kT)})\chi_{J_2j_2}] + [(e^{-2(J_{ST}/kT)})\chi_{j_3}]$$

where J_{ST} is the copper−copper intradimer interactions as defined by the Bleaney−Bowers equation (1). The $\exp(-2J_{ST}/kT)$ represents the population of the singlet and triplet states. Also,

$$\chi_{J_2j_2} = \frac{(2e^{-2(J_2/kT)} + 2e^{-2(j_2/kT)} + 10e^{2(J_2/kT)})N\beta^2g^2}{(e^{-4(J_2/kT)} + 3e^{-2(J_2/kT)} + 3e^{-2(j_2/kT)} + 5e^{2(J_2/kT)})kT}$$

where J_2 is the intradimer copper−nitroxide interactions, which can only occur at the higher temperatures as the triplet state of the copper dimer is populated; thus the $\exp(-2J_{ST}/kT)$ weighting factor is needed. The j_2 represents the intradimer nitroxide−nitroxide interactions, which should be ferromagnetic if each nitroxide is antiferromagnetically coupled to the triplet copper dimer. At the lower temperatures, where the singlet state of the copper dimer is most populated, $J_2 \rightarrow 0$ as the copper−nitroxide interactions no longer exist. Thus,

$$\chi_{j_1} = \frac{N\beta^2g^2}{(e^{-2(j_1/kT)} + 3)kT}$$

where j_1 is the intermolecular nitroxide−nitroxide interactions, which should be the only interactions at the lower temperatures as the nitroxides are not expected to interact intramolecularly through the singlet state copper dimer. This same fraction of the equation was also applied to the high-temperature fit, as there should be intermolecular nitroxide−nitroxide interactions at higher temperatures as well. Therefore,

$$\chi_{j_3} = \frac{N\beta^2g^2}{(e^{-2(j_3/kT)} + 3)kT}$$

where j_3 is the intermolecular nitroxide−nitroxide interactions at high temperatures, but j_3 should be different than j_1 as the nitroxides should now be coupled intramolecularly at high temperatures as well. For a more detailed analysis of the $\chi_{J_2j_2}$ term, see: Gruber, S. J.; Harris, C. M.; Sinn. E. *J. Chem. Phys*. **1968**, *49*, 2183.

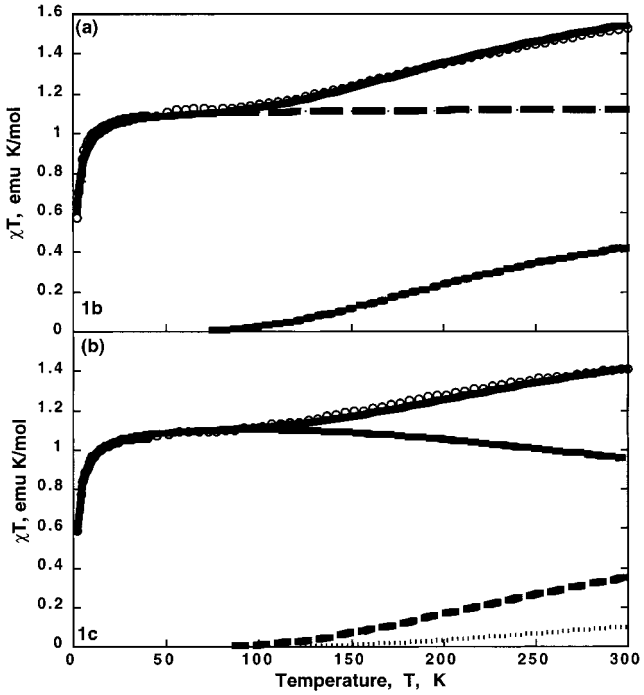

Figure 7. χT(T) for (a) $[Cu_2(O_2CMe)(NNBA)_3](EtOH)_2$, **1b**, and its fit to eq 4 with $n = 3$, $J_{ST} = -216$ K (-150 cm^{-1}), $g_{Cu} = 2.18$, $g_{org} = 2.001$, $\theta_S = -1.5$ K, and $\theta_T = -157$ K and (b) $[Cu_2(O_2CMe)(NNBA)_3]$-py_2, **1c**, with its fit to eq 4 with $n = 3$, $J_{ST} = -216$ K (-150 cm^{-1}), $g_{Cu} = 2.18$, $g_{org} = 2.001$, $\theta_S = -1.8$ K, and $\theta_T = -169$ K. The Bleaney−Bowers term of eq 4 is represented by dashed lines, the θ_S term by smaller dashes, the θ_T term by the dotted line, and the full fit by the solid line.

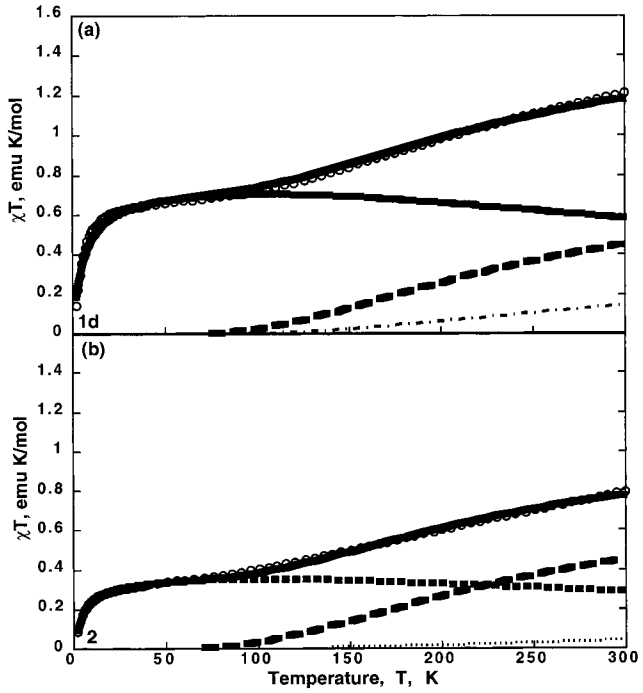

Figure 8. χT(T) for (a) $[Cu(O_2CMe)_2]_2(PYNN)_2$, **1d**, and its fit to eq 4 with $n = 2$, $J_{ST} = -223$ K (-155 cm^{-1}), $g_{Cu} = 2.18$, $g_{org} = 2.001$, $\theta_S = -5.8$ K, and $\theta_T = -5.8$ K and (b) $[Cu(O_2CMe)_2]_2(PYNN)$, **2**, and its fit to eq 4 with $n = 1$, $J_{ST} = -238$ K (-165 cm^{-1}), $g_{Cu} = 2.18$, $g_{org} = 2.001$, $\theta_S = -5.9$ K, and $\theta_T = -300$ K. The Bleaney−Bowers term of eq 4 is represented by dashed lines, the θ_S term by smaller dashes, the θ_T term by the dotted line, and the full fit by the solid line.

coupling between the $S = {}^1/_2$ ligands and the copper dimer triplet state ($\theta_S = -1.8$ K; $\theta_T = -169$ K) (Table 3).

As discussed above, after the reaction is allowed to proceed for 12 h, it is proposed that a linear chain of copper monomers is produced, **6b**, similar to that of the bromobenzoate monomers **6a**. As noted above, the susceptibility in this case can be modeled to Curie−Weiss behavior, eq 2, with $g_{Cu} = 2.16$ and a weak ferromagnetic coupling of $\theta = +0.7$ K (Figure 5b).

$[Cu(O_2CMe)_2(PYNN)]_2$, 1d. The addition of two PYNN radicals to the apical position of $[Cu(O_2CMe)_2]_2$, that is, $[Cu(O_2CMe)_2(PYNN)]_2$, **1d**, as observed for **1b** and **1c**, which differ by substituent, does not significantly alter the behavior of the dimer (Figure 8a), and the data are qualitatively similar to that observed for **1b** and **1c**; therefore the behavior was also modeled with eq 4.[25] The dimeric unit exhibits the singlet−triplet transition with $J_{ST} = -223$ K (-155 cm^{-1}), only slightly higher in energy with respect to **1b** and **1c**. Hence, in contrast to spin residing on a bridging carboxylate ligand [θ_T(**1b**, **1c**) ≈ -163 K], substantially weaker antiferromagnetic coupling ($\theta_T = \theta_S = -5.8$ K) is observed with a similar ligand axially bound to the copper dimer. Because $\theta_T = \theta_S$, it appears that only intermolecular interactions are present and the nitroxide does not couple to the triplet state of the dimer. The distant spin-bearing nitroxide moiety is probably twisted with respect to the pyridyl group and thus breaks the conjugation, reducing the coupling. Similarly poor, albeit ferromagnetic, coupling was reported for $[Ru(O_2CMe)_2]_2(PYNN)$.[13a]

$[Cu(O_2CMe)_2]_2(PYNN)$, 2. Addition of only 1 equiv of PYNN to $[Cu(O_2CMe)_2]_2$ results in the formation of chain-structured $[Cu(O_2CMe)_2]_2(PYNN)$, **2a** or **2b**, with χ(T) being fit to eq 4 with $J = -238$ K (-165 cm^{-1}), $g_{Cu} = 2.18$, $\theta_S = -5.9$ K, and $\theta_T = -300$ K (Figure 8b). The θ_S of -5.9 K is comparable to the -5.8 K observed for **1d**. However, direct copper(II)−nitroxide $Cu^{II}\cdots O$ interaction causes a significant increase in the antiferromagnetic interaction between the nitroxide and copper dimer triplet state compared to the discrete PYNN-pyridyl-capped dimers. The θ_T value of -300 K reflects strong antiferromagnetic coupling predominantly arising from direct interactions between the $S = {}^1/_2$ ligand and the triplet state of the copper dimer. Note that for **2b**, J is an average of the J values for two differently coordinated dimers.[21b]

In contrast to the Cu(II) dimer, which lacks metal−metal bonding, the spin coupling via related diamagnetic dimers with metal−metal bonding is substantially greater. Spins on aryl nitronyl and imidazolyl nitroxides axially bound to the $S = 0$ $[Rh^{II}(O_2CCF_3)_2]_2$ can interact intramolecularly through the Rh−Rh σ-bond,[14a,25] resulting in an observed nitroxide-only singlet−triplet transition, with $J = -120$ K (-84 cm^{-1}) for the phenyl nitronyl nitroxide (**4b**) substituted Rh(II) dimer. Likewise, strong coupling between nitroxides axially bound to $S = 0$ metal−metal quadruple-bonded $[Mo^{II}(O_2CCF_3)_2]_2$ has been reported for $[Mo^{II}(O_2CCF_3)_2(\mathbf{5})]_2$.[25] Thus, metal−metal bonding facilitates spin coupling via bypassing the poorer spin-coupling pathway of the carboxylate bridges as occurs for the Cu(II) dimers.[5]

In addition to the diamagnetic metal ion mediated nitroxide−nitroxide coupling, strong $S = 1$ $[Ru^{II}(O_2CCF_3)_2]_2$−nitroxide coupling has been reported for $[Ru^{II}(O_2CCF_3)_2(\mathbf{5})]_2$,[9c] ($J = -379$ K; -263 cm^{-1}), and slightly weaker $S = {}^3/_2$ $[Ru^{II/III}(O_2CCF_3)_2]_2$−nitroxide coupling has been reported for $[Ru^{II/III}(O_2CCMe_3)_2(\mathbf{5})]_2$ ($J = -187$ K; -130 cm^{-1}), although the strong withdrawing effect of the CF_3 with respect to the CMe_3 groups makes the former a stronger Lewis acid, resulting in stronger Ru−O bonding and spin coupling.[9c,22]

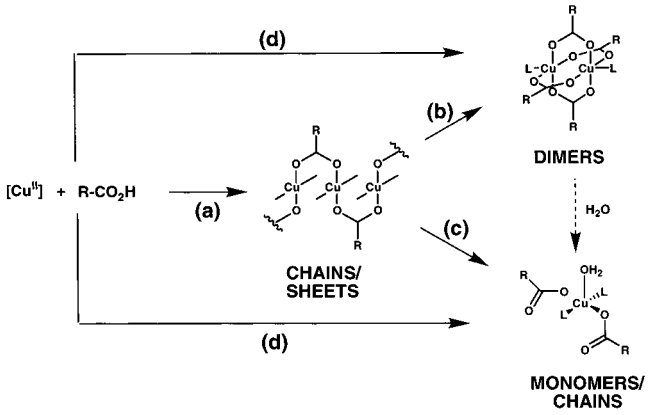

Figure 9. General mechanism for the formation of copper dimers and chains. (a) Reflux in xylenes or room temperature in ethanol. (b) Addition of 2 equiv of a capping ligand, L. (c) Addition of capping ligand and water, let stand. (d) Addition of multidentate carboxylate ligand, e.g., NNBA ligand.

Conclusion

In attempts to synthesize the copper carboxylate-based dimers, a general procedure for the pure dimers as well as linear chains was identified (Figure 9). Reaction of dimeric $[Cu(O_2CMe)_2]_2 \cdot 2H_2O$ with the acid of the desired carboxylate bridge leads to direct substitution (a). However, the product usually results in a chain structure, similar to those reported by Deakin et al.[19a] and Bakalbassis et al.[19b] Addition of a coordinating ligand to this chain compound, as a suspension or in solution, breaks apart the chains, and the ligand-capped dimers result (b). If water is present and the reaction is allowed to stand for long, the carboxylate bridges are broken and monomeric species (c) and in some cases ferromagnetically coupled one-dimensional chain structures form. An exception to this general mechanism may occur if a multidentate carboxylate-based ligand is utilized, such as PYNN, or when a coordinating solvent is used, as dimers may form (d).

The magnetic properties of these copper carboxylates vary with the type of structures formed. The singlet−triplet transition is still observed in all of the dimeric structures with J_{ST} ranging from −200 to −240 K (−140 to −170 cm^{-1}) characteristic of antiferromagnetic coupling. The singlet−triplet coupling is minimally altered by introduction of nitroxide-based radicals at either the bridging equatorial or terminal apical positions. However, direct coupling between the triplet copper dimer and the nitroxide is strongly antiferromagnetic, with stronger coupling observed for direct terminal coordination with respect to occupying bridging sites or for terminal coordination but with broken conjugation. The strong triplet Cu(II) dimer−nitroxide spin coupling has also been observed for related Ru(II) and Ru(II/III) dimer−nitroxide couplings.[9b,c,22] Furthermore, the Cu(II) dimers can be converted to hydrogen-bonded linear chains upon reaction with water, and these chains exhibit weak 1-D ferromagnetic coupling. Formation of chains composed of copper dimers bridged with the PYNN ligand leads to enhanced antiferromagnetic coupling.

Acknowledgment. The authors thank Drs. Laura Deakin, Jamie L. Manson, Kostantin I. Pokhodnya, Leigh C. Porter, and Professor Arthur J. Epstein (The Ohio State University) for their helpful discussions on the syntheses and magnetic properties of these compounds. Funding provided by the Department of Energy DMS (Grant No. DE FG 03-93ER45504) is gratefully acknowledged.

Supporting Information Available: The X-ray crystallographic files for $Cu(O_2CPh)_2(DMF)]_2$, **1a**, $[Cu(O_2CC_6H_4Br)_2py_2]\cdot H_2O$, **6a**, and $[Cu(O_2CPh)_2py_2]$, **7** in CIF format. This material is available free of charge via the Internet at http://pubs.acs.org.

IC0007106